thus neglect the higher order variations due to the polymer glass transition in our experiments. We measure the resonant wavelength shift for the oxide and polymer clad waveguides over a range of temperatures as is shown in Fig. (2).

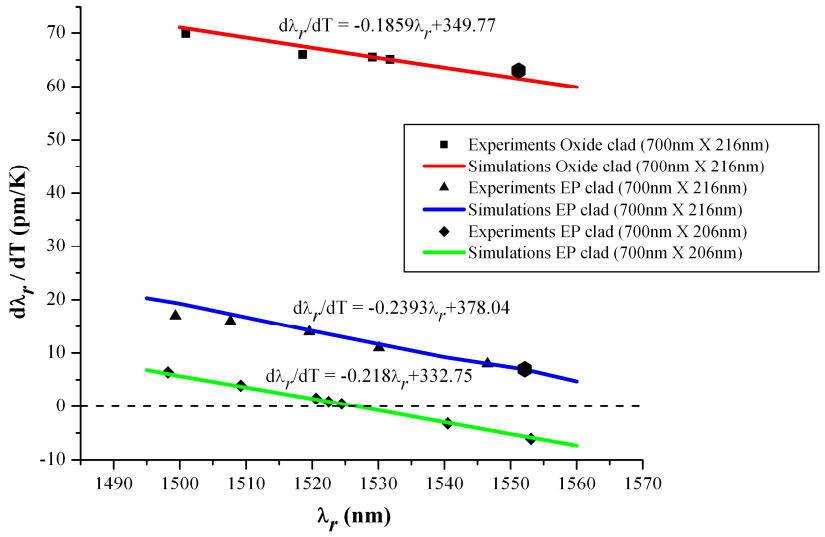

Fig. 2. Experimental results showing $d\lambda_r / dT$ variation with λ_r for TM mode propagation. The slope of the $d\lambda_r / dT$ variation with λ_r reflects the role of Γ (see Eq. (1), (2)) on TO and $d\lambda_r / dT$. Hence the wavelength at the dashed-line crossover point is an unique condition for $d\lambda_r / dT$ = 0. The hexagonal bold data points correspond to the spectral data shown in Fig. (1)

Figure (2) expresses the effects of both thermo-optic coefficient of the cladding and confinement factor on the resonance shift. The measurements for each resonant wavelength were carried out between 25°C-60°C and every data point is a linear regression of 8 data points taken at every 5°C interval. For large resonance shifts (TDWS > 10pm/K), $R^2 \geq 0.99$, and for near athermal performance (TDWS ≤ 1pm/K) $R^2 \geq 0.94$ due to reduced linear correlation arising from the residual second order terms discussed below. The dramatic decrease of TDWS from 65 pm/K for an oxide cladding to as low as 0.5pm/K at 1524nm for the EP polymer cladding can be attributed to the negative thermo-optic coefficient of the polymer and its effect on the effective thermo-optic coefficient of the system. Figure 2 demonstrates two important results: i) the achievement near perfect thermo-optic compensation, and ii) a variation of TDWS with wavelength that correlates well with simulated values. As explained earlier and as verified by the coincidence between data and simulation, the variation in confinement factor with wavelength changes the TDWS. The excellent agreement between experimental data and the simulations clearly validates our theoretical formulation of TDWS in Section 2.

#128874 - $15.00 USD Received 24 May 2010; revised 18 Jul 2010; accepted 20 Jul 2010; published 2 Aug 2010
(C) 2010 OSA

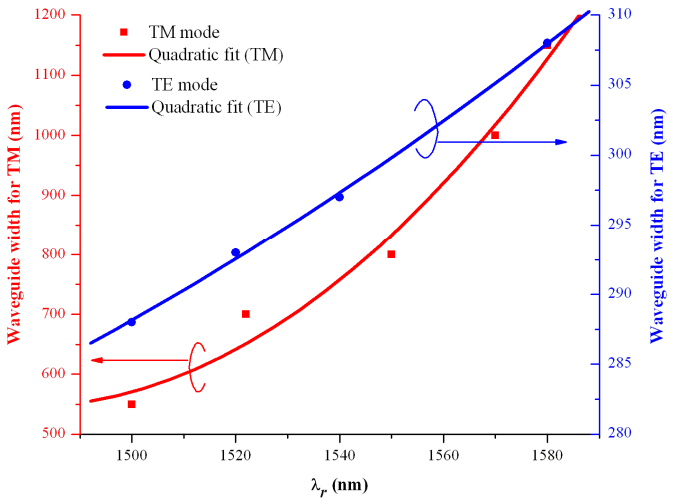

Fig. 3. Variation of athermal waveguide width with wavelength for TE and TM modes. These simulation results are for an a-Si waveguide of 206nm height with an SiO_2 underclad and the EP polymer over-cladding. The desired waveguide width for athermal operation increases with wavelength to keep the confinement factor constant, consistent with the theory presented in section 2.2.

The wavelength dependence of TDWS imposes an additional design constraint of different waveguide dimensions for different resonant wavelengths to achieve athermal operation. For a single WDM implementation, the mask design should incorporate varying waveguide widths, for instance, when the height of the waveguide (layer thickness) is fixed. Figure 3 plots the range of the wavelength dependent variation in waveguide dimensions for athermal operation of both TE and TM modes. The simulation assumes an a-Si ring with an oxide under-cladding and a polymer over-cladding. We fix the height of the a-Si waveguide at 206nm and calculate the desired width, to achieve a peak shift of less than 0.5pm/K, at various wavelengths. The desired width varies from 550nm (at 1500nm) to 1150nm (at 1580nm) as the wavelength increases. Such a large variation in waveguide width can be correlated to the small dependence of the confinement factor of a TM mode on width compared to height variation. Conversely, one can expect to achieve athermal operation of a TE mode over a smaller range of widths for a given range of wavelengths. Figure (3) clearly shows this stronger dependence of confinement factor of a TE mode on the width of the waveguide. Figure (3) also defines the 'athermal constraint' on fabrication tolerance, since changes in the waveguide width can shift athermal operation to a different wavelength. As an example, an error of 100nm in the waveguide width would shift the "athermal response peak" by 10nm.

Residual second order variations are revealed when TDWS is small. Figure (4) shows the experimental variation of resonant wavelength with temperature for a 700nm × 206nm a-Si waveguide with an EP cladding.

#128874 - $15.00 USD Received 24 May 2010; revised 18 Jul 2010; accepted 20 Jul 2010; published 2 Aug 2010
(C) 2010 OSA

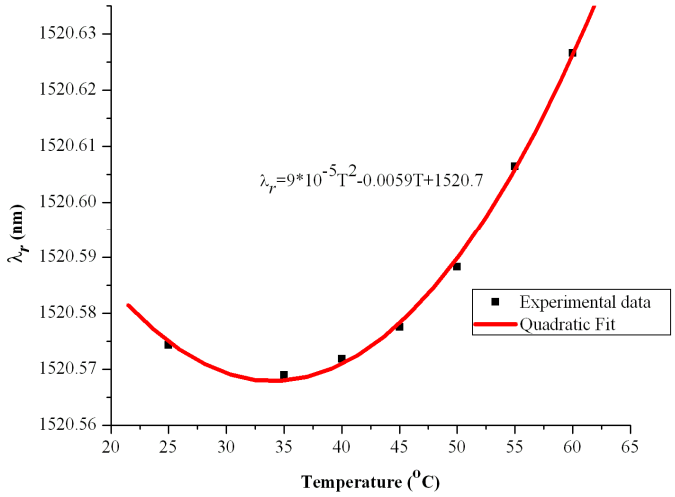

Fig. 4. Measured second order variations of resonant wavelength with fit to a quadratic dependence. The residual second order effects become important when the first order terms vanish at low peak shifts (<2pm/K). The quadratic term has contributions from the temperature dependence of the confinement factor and from the second order material coefficients.

The residual quadratic term seen in experiments ($9 \times 10^{-5} \pm 1 \times 10^{-5}$nmK^{-2}) is of the same order of magnitude predicted in the simulation ($2 \times 10^{-5} \pm 1 \times 10^{-6}$ nmK^{-2}). The higher value of the experimental second order term compared to simulation suggests a significant contribution from the second order material coefficients, $\frac{\partial^2 n_c}{\partial T^2}$ and $\frac{\partial^2 n_{cl}}{\partial T^2}$, that we neglected in the simulations (first 2 second order terms in Eq. (3)). The first 2 second order terms of Eq. (3) can be calculated based on our the experimentally measured second order term, and a value of $4 \times 10^{-7} \pm 1 \times 10^{-7}$K^{-2} for the second order material coefficient of the waveguide system (in other words, second order effective material TO coefficient) results. Cocorullo et al. [14] have reported that the second order thermo-optic coefficient of a-Si is roughly 1.43×10^{-6}K^{-2}, so the determined value is in a reasonable range for the polymer clad system.

5. Material selection for high density integration: Si rings vs Si_3N_4 rings

The motivation behind using Si ring resonators for WDM filter applications arises from its high-index contrast and high mode confinement. As a result, Si rings can have small bending radii resulting in large FSR. However, athermal operation of these rings requires reduced confinement ($\Gamma = 0.58$) for the mode to penetrate the cladding. The result is a lower effective index (1.78) waveguide with higher radiative bending loss. This design rule leads one to inquire whether a lower-index contrast (LIC) waveguide core material with a lower TO coefficient, such as Si_3N_4 (TO = 4×10^{-5}), would perform as well or better for athermal WDM applications. We use bend radius (R_b) as a variable in the figure of merit for the ring resonator, and we calculate for TM mode to be consistent with our experimental results. We start the comparison by finding the confinement factor required for athermal operation of nitride rings with the same polymer cladding used for a-Si rings. We then proceed to find the bending radius for both Si and Si_3N_4 for a given bending loss [15], which we fixed at 4.34dB/cm (or 1cm^{-1}).

Table 2 summarizes R_b for both systems. As the results show, the advantage of high-index contrast (HIC) (a-Si) is neutralized under the constraint of athermal operation, and the R_b

#128874 - $15.00 USD Received 24 May 2010; revised 18 Jul 2010; accepted 20 Jul 2010; published 2 Aug 2010
(C) 2010 OSA

performance is similar to the lower-index Si_3N_4 core. Therefore, materials selection of lower index contrast systems like Si_3N_4 might prove advantageous, since the lower TO coefficient may allow the use of a wider range of commercially available polymers to achieve athermal behavior. Si_3N_4 rings have a higher FSR due to their smaller group index (n_g), and they could prove additionally useful for athermal WDM applications where FSR is the primary performance driver. When developing scaling rules for the material selection for athermal performance, it is important to realize that HIC systems lose their benefits over LIC systems in terms of small R_b and high FSR, and the two performances becomes comparable.

Table 2. Performance comparison of two athermal waveguide designs, for an a-Si core and a Si_3N_4 core, with the same EP polymer overclad

Material	n	Γ	n_{eff}	n_g	R_b(microns)
Si	3.48	0.58	1.78	3.68	3.5
Si_3N_4	2.05	0.9	1.75	2.2	5.5

6. Summary and conclusion

We develop the design principles for athermal waveguide device performance. We demonstrate prototype ring resonators with near complete thermo-optic compensation of an a-Si on SiO_2 waveguide using a polymer cladding. We measure a resonant wavelength shift of 0.5pm/K, which is the lowest TDWS value reported to date for silicon resonators. The design formalism and prototypes establish the requirement for a unique waveguide dimension for each operating wavelength. The athermal resonator performance reveals residual second order terms that are also described in the theoretical section. This report validates a general solution for temperature-independent performance of silicon resonant photonic devices. An evaluation of the performance tradeoffs of athermal HIC systems in terms of FSR and bend radius shows that LIC systems might be superior to HIC systems in certain applications.

Acknowledgement

We acknowledge Dr. Ningning Feng of Kotura for support with simulations for bending loss calculations. This work is sponsored under the Defense Advanced Research Projects Agency's Athermal Photonic Circuits (APhoCs) program. The program is executed by the Microsystems Technology Office (MTO) under Award No. W911NF-09-1-0059, Program manager: Mike Haney.

#128874 - $15.00 USD Received 24 May 2010; revised 18 Jul 2010; accepted 20 Jul 2010; published 2 Aug 2010
(C) 2010 OSA